FFI-rapport 2012/00267

Transport and dispersion of non-neutral toxic industrial chemicals in an urban environment

Emma Wingstedt, Thomas Vik and Bjørn Anders P. Reif

Norwegian Defence Research Establishment (FFI)

31 August 2012

FFI-rapport 2012/00267

1149

P: ISBN 978-82-464-2117-9
E: ISBN 978-82-464-2118-6

Keywords

Spredning

CFD

Ikke-nøytral gass

Urbant miljø

Approved by

Monica Endregard	Project Manager
Jan Ivar Botnan	Director

English summary

The main focus in this study was to investigate the difference between the dispersion and transport process of non-neutral and passive gas release, respectively, in an urban area. The method used was the LES approach, which previously has shown good results for urban dispersion of neutral gas. Chlorine and ammonia were chosen as non-neutral gases, where chlorine is a heavier-than-air gas while ammonia is a lighter-than-air gas. Both chemicals are usually stored and transported in their respective liquid form in pressurized tanks. Hence, the source was estimated to imitate a rupture from that kind of container. That means that both the liquid and vapor state of the chemicals were released, and that the subsequent evaporation process was included in the calculations.

The results yielded a significant difference between the evaporation of chlorine and ammonia, where chlorine evaporated quickly whereas liquid ammonia did not. A possible explanation for this lies in the latent heat of evaporation. This difference led to a considerable disparity between the sources where chlorine could be assumed to be released from a point source, while ammonia gas evaporated from a much larger area. This affected the subsequent transport and made it hard to compare the two cases of non-neutral gases with each other. Since the neutral case only considers release of gas from a point source, the dispersion of neutral gas can only be compared to transport of chlorine in this study.

The results also indicate that the heavier-than-air gas is not as affected by vertical mixing as the neutral gas. This gives a plume that do not reach as high, but as time progresses spread more horizontally as compared to the passive scalar. The latter is most likely due to the channeling effects caused by building structures. An analysis of the temperature field confirms a rapid evaporation of the liquid chlorine. No liquid pool was observed and the vaporized chlorine quickly reached the same temperature as the surrounding air.

In the ammonia case, not only the gaseous phase, but also the liquid droplets were transported. Liquid ammonia covered a large area around the original source, which gave rise to a secondary evaporation and, hence, a larger release area for ammonia gas. Due to a density lower than the density of air, an increased wind velocity was seen where the concentration of vapor ammonia was high. This also increased the mixing yielding a higher, but also a more diluted, plume. The dispersed ammonia stayed cold for a longer period of time compared to chlorine, and the temperature in a larger area was affected.

Sammendrag

Målet med denne studien var å undersøke forskjellen mellom spredningsprosessen av ikke-nøytral og passiv gass i et urbant område. Metoden som ble brukt var LES-modellen, som tidligere er vist å gi gode resultater for urban spredning av nøytral gass. Industrikjemikaliene klor og ammoniakk ble valgt som ikke-nøytrale gasser, der klor er tyngre enn luft mens ammoniakk er lettere enn luft. Begge kjemikaliene oppbevares og transporteres vanligvis i flytende form i trykksatte tanker. Kilden til utslippet ble derfor valgt å være et brudd i en slik beholder, hvilket betyr at både væske og damp ble sluppet ut, og at fordamping ble inkludert i beregningene.

Resultatene viste en betydelig forskjell mellom fordamping av klor og ammoniakk, der klor fordampet raskt mens flytende ammoniakk ikke gjorde det. En mulig forklaring til det kan være ulikheten i latent varme. Denne forskjellen førte videre til at kildene til gassutslippet ble ulikt i de to scenarioene. Klorgass kan antas å bli sluppet fra en punktkilde mens ammoniakk fordampet fra væskeansamling over et mye større område. Dette påvirket den videre transporten og gjorde det vanskelig å sammenligne de to tilfellene av ikke-nøytral spredning. Siden nøytral gass bare slippes fra en punktkilde i disse simuleringene, kan den her bare sammenlignes med spredningen av klor.

Resultatene indikerte også at gass som er tyngre enn luft ikke påvirkes like mye av den vertikale miksingen som nøytral gass. Dette gir en sky som ikke når like høyt, men som etterhvert spres mer i horisontalplanet i forhold til en passiv skalar. Det sistnevnte er mest sannsynlig på grunn av kanaliseringseffekter forårsaket av bygningene. En analyse av temperaturfeltet bekrefter en rask fordamping av flytende klor. Det ble heller ikke observert noen væskeansamling på bakken, og klor i gassform nådde raskt samme temperatur som luften rundt.

I tilfellet med ammoniakk ble både gassfasen og væskefasen transportert. Flytende ammoniakk dekket et stort område rundt den opprinnelige kilden og ga opphav til en sekundær fordamping og dermed et større utslippsområde for ammoniakkgass. En økt vindhastighet er observert i områdene der konsentrasjonen av ammoniakkdamp er høy, hvilket også innebærer at tettheten er lavere enn tettheten for luft. Dette gir en økt miksing, som igjen leder til en høyere, men også en mer fortynnet sky. Ammoniakken holder seg kald en lengre periode sammenlignet med klor, og temperaturen er påvirket i et større område.

Contents

Preface

Visualizations of the simulations presented in this report can be obtained by contacting the Protection Division at the Norwegian Defence Research Establishment.

1 Introduction

There are increased concerns about release and aerial dispersion of toxic industrial chemicals (TIC) due to industrial accidents and terrorist activities since it may threaten the lives and health of an urban population. Predicted spatial patterns and time variations of TIC concentrations are needed by emergency responders and responsible authorities in order to estimate the consequences and to identify most effective countermeasures to limit the impact. Dispersion of non-neutral TIC, especially in a complex urban environment, poses severe challenges and is an important area of research. In this study both chlorine and ammonia have been considered. The terminology "non-neutral" alludes to the fact that chlorine is a heavier-than-air gas, while ammonia is a lighter-than-air gas. Both are usually stored and transported in their respective liquid state, but when they come in contact with the atmosphere they evaporate due to their low boiling temperature of approximately 239 K.

The transport and dispersion of contaminants in the atmosphere are governed by the conservation laws of mass, momentum, and energy. Since both chlorine and ammonia are non-neutral gases, they will predominantly be transported with the wind field, but the transport may also be significantly affected by the density differences, heat exchange, and gravitational force. The density difference may severely alter the turbulence field due to the resulting stably or unstably stratified background. The impact of the stratification primarily modifies the vertical mixing process of the plume, and therefore also the overall transport process. A neutral gas, i.e., a gas with the same density as air, on the other hand will be transported with the wind field without affecting its dynamics. In both cases it is the wind field that is the most important dynamical process, and in order to model the dispersion successfully, it is crucial to accurately model the wind field.

In urban environments the dominating effects on the flow field are kinematic blocking of velocity components normal to solid surfaces and non-local effects caused by pressure reflections (cf. e.g., (Durbin and Reif, 2002)). The non-local effects dominate in the atmospheric boundary layer (ABL) where they modify the turbulence anisotropy yielding a change in the dispersion process. The kinematic blocking dominates the local flow conditions in built up areas, where buildings cause street canyon effects, flow separation and generation of unsteady wakes.

Due to a steadily increasing computer capacity, Computational Fluid Dynamics (CFD) has become a popular tool for modeling dispersion. However, a number of modeling issues need to be addressed in order to warrant the use of CFD in urban areas (Lee et al., 2000). Many urban dispersion studies are based on the assumption that the flow field is statistically steady and therefore the steady state Reynolds-averaged Navier-Stokes (RANS) method is widely used (see e.g., (Coirier et al., 2005; Lien and Yee, 2004; Lien et al., 2006; Santiago et al., 2007)). However, results show that even though the mean velocity field can be fairly well predicted with this method, the turbulence kinetic energy is in general underpredicted, which may lead to a poorly predicted mixing process.

A number of studies regarding numerical simulation of dense gas dispersion using the Unsteady RANS (URANS) approach have been carried out in the past (McBride et al., 2001; Perdikaris and Mayinger, 1994; Sklavounos and Rigas, 2004) with fairly good results. The URANS method inherently assumes the mean flow field to be statistically unsteady, an assumption better suited for flow in an urban environment due to bluff body shedding downstream building structures. Another approach that naturally includes the flow unsteadiness is Large Eddy Simulation (LES), which resolves the inherent unsteadiness of the large scale turbulence irrespectively of the nature of the averaged flow field. Previous studies using the LES approach for urban dispersion modeling of neutral gases have shown good results, especially in the near-surface layer (Fossum et al., 2012; Liu et al., 2011).

The objective of the present study is conducting a parametric study to investigate the difference between the dispersion and transport processes of non-neutral and passive gas releases, respectively, in an urban environment with realistic complexity.

2 Mathematical Modeling

In this study, the LES method has been used, in which the three-dimensional time dependent filtered Navier-Stokes equations are solved numerically. The small (sub-grid) scale turbulence can not be resolved and must therefore be modeled. For a Newtonian, incompressible flow, the filtered equations for conservation of mass and momentum are given by

$$\frac{\partial \bar{u}_i}{\partial x_i} = 0, \tag{2.1}$$

$$\frac{\partial \bar{u}_i}{\partial t} + \bar{u}_j \frac{\partial \bar{u}_i}{\partial x_j} = -\frac{1}{\rho}\frac{\partial \bar{p}}{\partial x_i} + \nu \frac{\partial^2 \bar{u}_i}{\partial x_j \partial x_j} - \frac{\partial \tau_{ij}}{\partial x_j} + g_i. \tag{2.2}$$

Here, $\bar{u}_i(\mathbf{x}, t)$ and $\bar{p}(\mathbf{x}, t)$ denote the spatially filtered velocity component in the x_i-direction and the filtered kinematic pressure, respectively. ν is the kinematic viscosity, ρ the density and g_i is the gravitational force in the x_i-direction. $\tau_{ij} = \overline{u_i u_j} - \bar{u}_i \bar{u}_j$ is the sub-grid scale stress tensor which represents the effect of the unresolved small scale fluctuations on the resolved large scale motion. This term is *a priori* unknown and needs to be modeled. In the present study the dynamic Smagorinsky model is used. It can be written as

$$\tau_{ij} = \frac{1}{3}\tau_{kk}\delta_{ij} - 2\bar{\Delta}^2 |\bar{S}| \bar{S}_{ij}, \tag{2.3}$$

where $\bar{S}_{ij}$ is the filtered rate-of-strain tensor and $|\bar{S}| \equiv (2\bar{S}_{ij}\bar{S}_{ij})^{1/2}$. The filter length scale is given by $\bar{\Delta} = min(\kappa d, C_s V^{1/3})$, where κ is the von Kármán constant, d is the distance to the closest wall and V is the volume of the computational cell. The Smagorinsky model constant, C_s, is dynamically computed based on the information provided by the resolved scales of motion (Fluent 6.3 User's Guide).

Since dispersion of a non-neutral gas is considered, the temperature field also needs to be modeled. The filtered energy equation is given by

$$\frac{\partial(\rho\bar{E})}{\partial t} + \bar{u}_j \frac{\partial\left(\rho\bar{E}+\bar{p}\right)}{\partial x_j} = \frac{\partial}{\partial x_j}\left(k_{eff}\frac{\partial T}{\partial x_j}\right) + \bar{u}_j \frac{\partial \tau_{eff}}{\partial x_j} + \nabla\cdot\left(\sum_i h_i J_i\right), \quad (2.4)$$

where k_{eff} is the effective thermal conductivity and J_i is the diffusion flux of specie j. The terms on the right hand side of the equation represent energy transfer due to conduction, viscous dissipation and species diffusion, respectively.

In the case with non-neutral gas dispersion, both liquid and vaporized chlorine, and ammonia, are released into the environment. Since both chemicals have a boiling point of approximately 239K it is anticipated that their liquid state will evaporate quickly, but since the process occurs within a finite time this effect must also be modeled. Here, the evaporation of liquid chlorine and ammonia is calculated from a heat balance equation

$$Q_{air} + Q_{Cl_2/NH_3} - Q_L = 0, \quad (2.5)$$

where Q_{air} is the heat released due to the temperature difference between the final temperature of the liquid/vapor mix, T_f, and the ambient air temperature given by the energy equation, T. Q_{Cl_2/NH_3} is the heat due to the temperature difference between the boiling temperature of chlorine and ammonia, T_b, and T_f, and Q_L is the heat taken up by the evaporation of liquid chlorine and ammonia

$$Q_{air} = n_{air}C_{p,air}(T - T_f), \quad (2.6)$$
$$Q_{Cl_2/NH_3} = n_{Cl_2/NH_3}C_{p,gas}(T_b - T_f), \quad (2.7)$$
$$Q_L = n_{Cl_2/NH_3}L_{Cl_2/NH_3}. \quad (2.8)$$

Here, n denotes the molar concentration, C_p the heat capacity and L_{Cl_2/NH_3} the latent heat of evaporation of chlorine and ammonia, respectively. By solving equation (2.5), the temperature of the liquid/vapor mix is obtained which is subsequently used to calculate the density of the mixture using the ideal gas law. The density of the mixture is calculated in each computational cell by a user defined function and is used in the equation describing dispersion of different species (Eq.(2.9)).

The dynamical process governing the transport and mixing of a specie is described by a convection-diffusion equation given by

$$\frac{\partial\bar{Y}_i}{\partial t} + \bar{u}_j\frac{\partial\bar{Y}_i}{\partial x_j} = \left(D_{i,m} + \frac{\bar{\Delta}^2|\bar{S}|\rho D_{i,t}}{\mu_t}\right)\frac{\partial^2\bar{Y}_i}{\partial x_j^2}, \quad (2.9)$$

where $\bar{Y}_i$ is the local mass fraction, and $D_{i,m}$ and $D_{i,t}$ are the molecular and turbulent diffusivity, of a specie i, respectively. The right hand side of the equation represents the mass diffusion, which includes both the molecular and turbulent diffusivity. Equation (2.9) is solved for each specie introduced in the computation. For the non-neutral gas simulations that means it is solved for both liquid and vaporized chlorine and ammonia, respectively, whereas in the case with a neutral gas release it is solved for a scalar with identical physical properties to that of air.

3 Numerical approach

The pressure based solver in Fluent 12.0 (Fluent 6.3 User's Guide) is used for the numerical simulations. Spatial derivatives are discretized using a second order upwind scheme and a second order implicit Euler formula is employed for the time integration. For the pressure-velocity coupling, the SIMPLE algorithm is used. A time step corresponding to an estimate of the time scale for the large scale turbulence, i.e., $\Delta t = \tau = L/U = 0.1\ s$, is used.

A central part of Oslo city is chosen to represent a realistic urban area (Figure 3.1). The area, in total $1300\ m$ x $900\ m$ x $300\ m$, is discretized into approximately $75 \cdot 10^6$ cells, where the smallest cells are located in close proximity of the release point (see Figure 3.2). The global wind direction is in the x-direction (i.e., from west to east), y is the spanwise direction and z is the ground-normal direction. In order to obtain a realistic incoming boundary layer profile, a simplified simulation

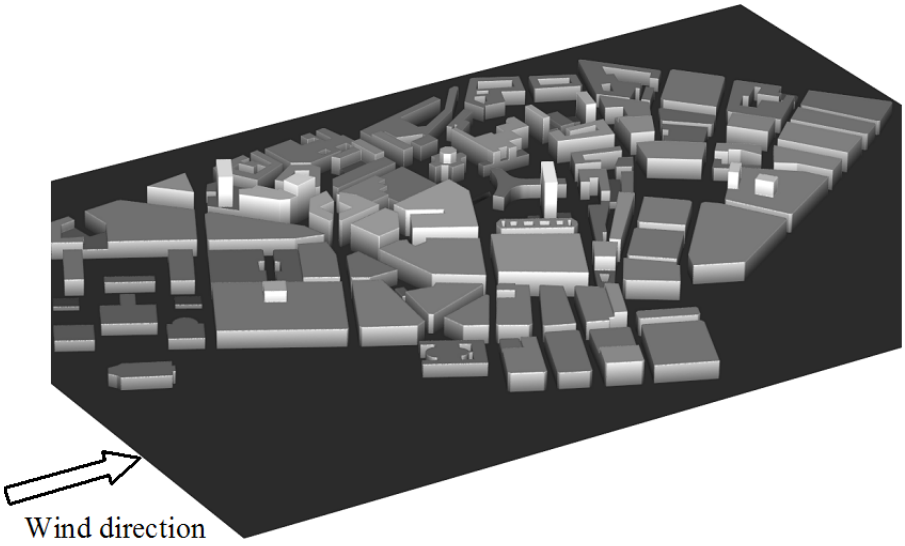

Figure 3.1 An overview of the computational domain with dimensions 1300 m x 900 m x 300 m.

methodology was used with a constant wind speed of $3\ m/s$. The results, in terms of velocity components in each spatial direction stored in the outflow plane, was then used as an input for the LES simulation. This simulation was subsequently run for approximately one flow through time, i.e., the time corresponding to the time a particle would use to be transported from one side of the computational domain to the other. In this case that corresponds to $1300\ m/3\ ms^{-1} \approx 40\ s$. The velocity components on the outlet boundary was then used as inlet velocity boundary

condition for the rest of the simulations. Also, a spectral synthesizer method was used to generate turbulence fluctuations. The outlet and lateral boundaries are defined as a pressure outlets with no temperature gradient and at the top of the domain symmetry conditions are prescribed. The symmetry boundary is sufficiently far away from the area of interest so that any influence of the symmetry assumption is negligible on the solution. Both the ground and all the building surfaces are defined as no-slip walls with zero heat flux. It is assumed to be an isothermal environment, with a constant temperature of $288.15\ K$. In the dense gas simulation, a mixture containing 85%

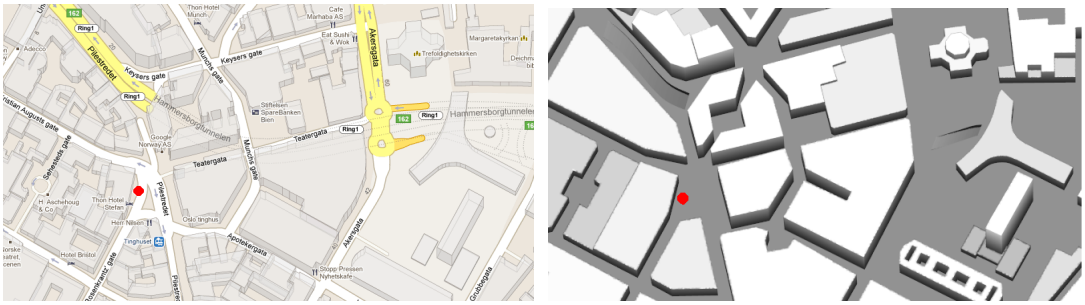

(a) Source location on map (b) Source location in the geometry

Figure 3.2 Comparison between map of urban area and the computational geometry. The red dot in both figures represent the source location 1 m above ground level.

liquid and 15% vaporized chlorine are released from a pressurized tank close to the ground (see Figure 3.2). The mass-flow was estimated to $33.3\ kg/s$ and the release continuous for $60\ s$, during which 2 tonne of the chlorine mixture is discharged. The temperature of the released mixture is set to $239.05\ K$. Neutral gas dispersion was simulated by releasing a specie with the same physical properties to that of air. To be able to compare the results one-to-one to the non-neutral cases, the same volume of passive gas was released, yielding a mass-flow of $7\ kg/s$. The release time was set the same as for the chlorine case. In the lighter-than-air gas simulation, a mixture of liquid and vaporized ammonia was released in the same proportions as in the dense gas case. The same release time and mass flow was also used. The temperature of the ammonia mixture is $239.65\ K$.

4 Results and discussion

The simulations yielded a significant difference between the two releases of non-neutral gas. In the chlorine case, the evaporation was quick and when the discharge of liquid/vapor mixture stopped all liquid chlorine had already evaporated. This means that only dense chlorine gas was transported and that the source can be assumed to be a point source. Hence, it can easily be compared to the neutral gas release where only a gaseous state is released.

Ammonia, on the other hand, showed a different behavior. Here, a liquid pool was formed on the ground which gave rise to a secondary evaporation from a much larger area compared to a point source. Therefore, it is difficult to compare the transport of ammonia with the other cases. The discharges, however, including the effect on both wind speed and temperature, may be compared.

4.1 Chlorine release

As already mentioned, it is the wind field that is the most important dynamical process when it comes to dispersion as long as the wind speed is sufficiently high. In an urban area, like the one chosen here, the kinematic blocking in addition to unsteady meandering caused by the massively separated regions downstream buildings dominate the wind field characteristics. Figure 4.1a displays contours of the instantaneous streamwise velocity in a plane parallel to the ground at $5\ m$ height. It is clearly seen that the blocking causes large flow separation regions and that the flow field is extremely complex.

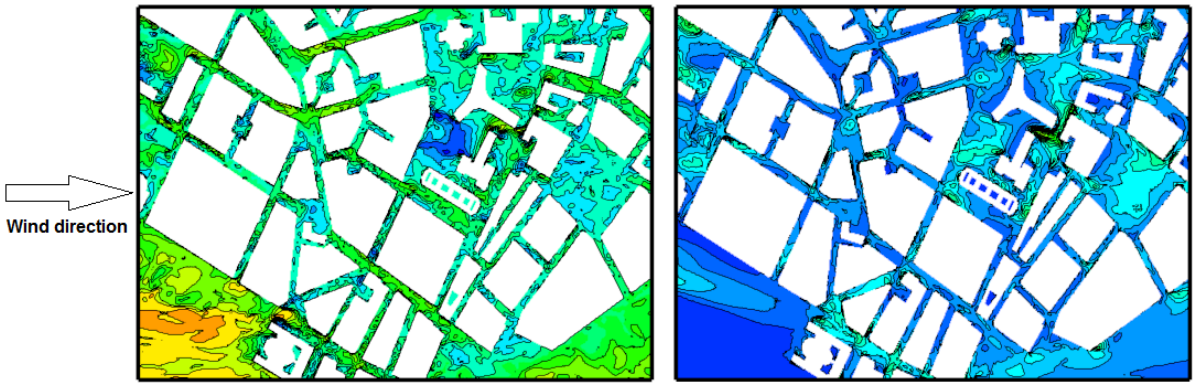

(a) Streamwise velocity.
Red $\approx 3.5\ m/s$ and blue $\approx -1.7\ m/s$

(b) Turbulence kinetic energy.
Green $\approx 0.65\ m^2/s^2$ ans blue $\approx 0\ m^2/s^2$

Figure 4.1 Instantaneous quantities in a plane parallel to the ground at $5\ m$ *height*

The instantaneous turbulence kinetic energy in the same plane, $5\ m$ above the ground, is seen in figure 4.1b. Not surprisingly the complexity of the flow field is easily recognized here as well.

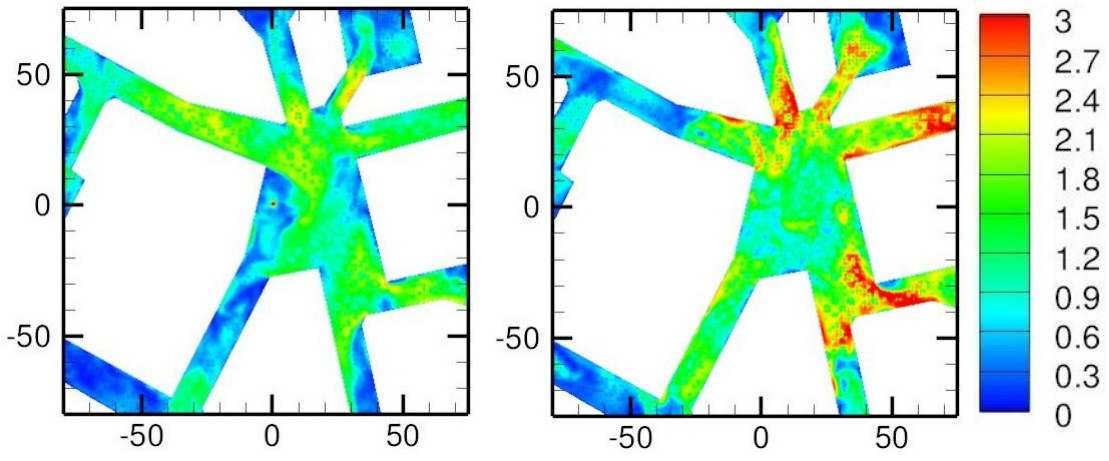

(a) Passive release

(b) Chlorine release

Figure 4.2 Velocity magnitude in the area around the source after $60\ s$ *release*

Figure 4.2 shows the velocity magnitude in the area around the release point after $60\ s$ release of (4.2a) passive gas and (4.2b) chlorine mixture. As seen, there are significant differences between

the two wind fields. This is due to the density difference between the passive gas and the dense chlorine. In the case with passive release, the surrounding wind is not affected by the density of the gas. That is however the case with the heavy gas release, where the dense chlorine mixture suppress the wind velocity in the area with high density (see figure 4.3a).

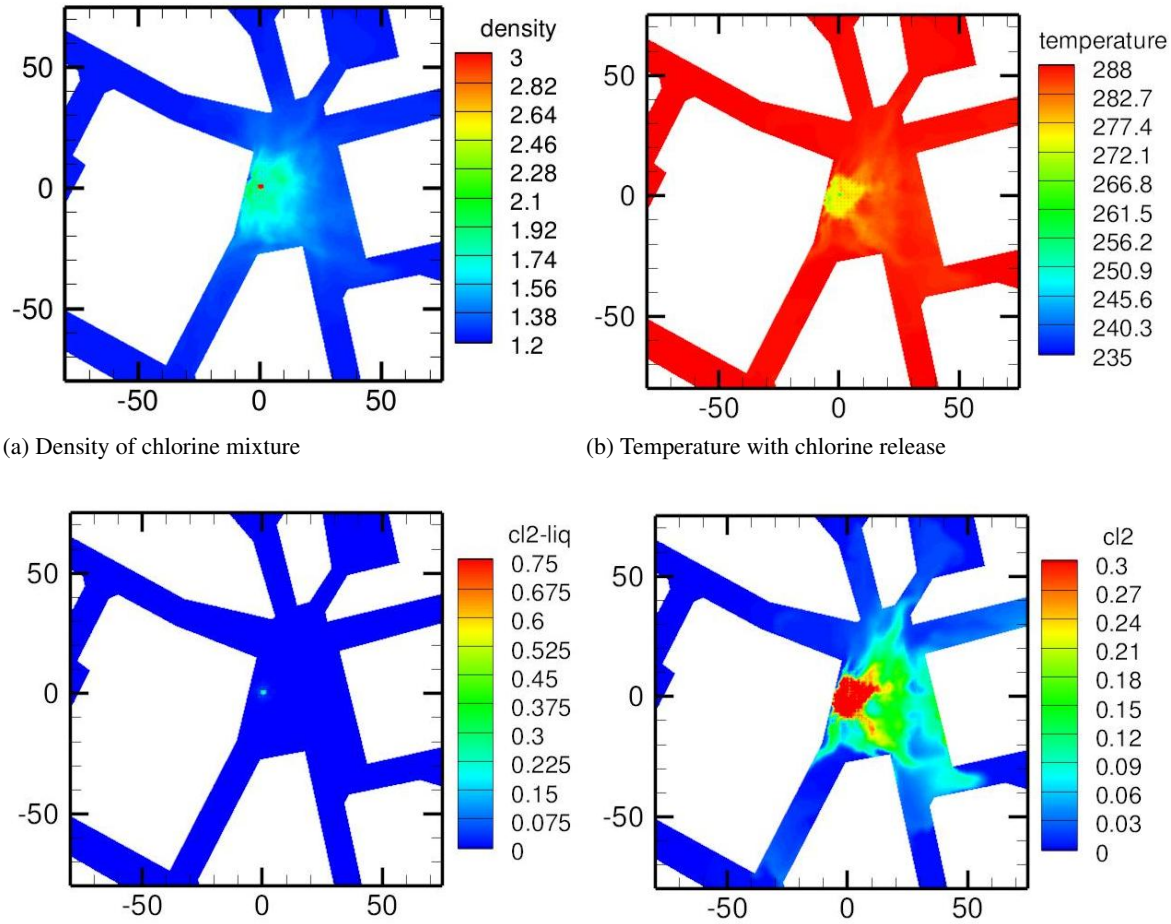

(a) Density of chlorine mixture

(b) Temperature with chlorine release

(c) Concentration of liquid chlorine

(d) Concentration of vaporized chlorine

Figure 4.3 Density and temperature, as well as concentration of liquid and gaseous chlorine, in a plane parallel to the ground at $1\ m$ *height after* $60\ s$ *release*

The temperature of the released chlorine mixture is lower than the ambient air temperature. Figure 4.3b shows the temperature field, $60\ s$ after the release of chlorine started, in a plane parallel to the ground at $1\ m$ height. It is seen that even though large amounts of cold chlorine is released, the temperature field is only affected in close proximity to the release point. Also, even though the temperature of the release is $239\ K$, the lowest temperature in the area is approximately $260\ K$. Hence, the temperature of the released mixture is quickly increased to a point above the boiling temperature of chlorine, indicating a rapid evaporation of the liquid state. Figure 4.3c shows the concentration of liquid chlorine after $60\ s$, i.e., when the release stops, and it is easily seen that only a small area contains any liquid. In Figure 4.3d the concentration of the gaseous state of chlorine is seen, with the highest values closest to the source. Comparing figure 4.3b to figure 4.3d

it is seen that the temperature is lower where there is high concentration of vaporized chlorine, but also that a large amount of the vapor has reached the ambient air temperature already after 60 s.

4.1.1 Comparison between release of chlorine and neutral gas

The concentration data presented in this section is taken from within the first 120 s of the simulations, i.e., up to one minute after the releases stop. All the data have been normalized with its respective maximum value, hence no conclusions can therefore be made about the dilution of the plume. All contour plots show spatially averaged concentration in different planes, i.e., the data have been averaged over one direction (see figure 4.4). The release point is located at $x = y = z = 0$. Note the different scales on the axis for different times.

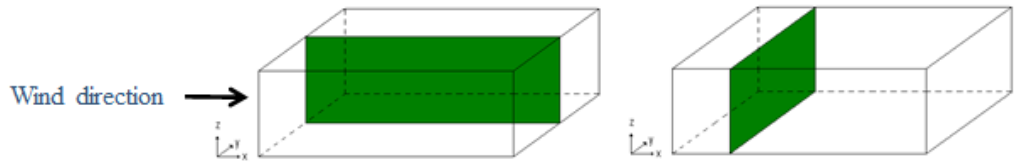

(a) Planes of streamwise averaging (b) Planes of spanwise averaging

Figure 4.4 Direction of averaging

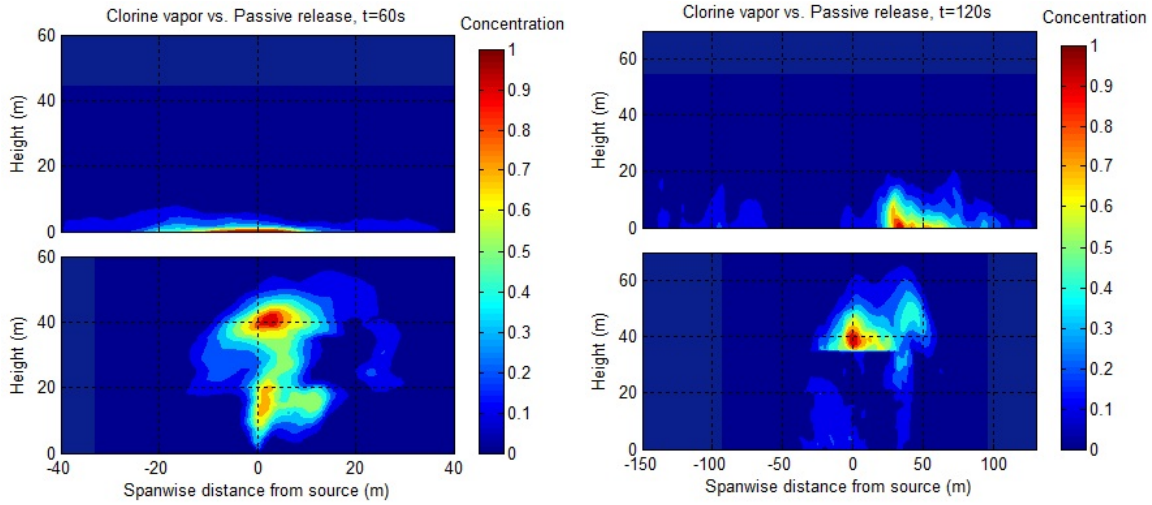

(a) Concentration in a xz-plane at $t = 60s$ (b) Concentration in a xz-plane at $t = 120s$

Figure 4.5 Spatially averaged (in streamwise direction) concentration of chlorine vapor (above) and passive scalar (below)

Figure 4.5 displays the spatially averaged concentration in a xz-plane, thus reveling the spanwise extension of the plume, at $t = 60$ s (Figure 4.5a) and $t = 120$ s (Figure 4.5b). The pictures on top show the chlorine vapor and the pictures below the passive release. The most noticeable difference between the two gases is the height of the plume. The heavy gas reaches a height of approximately 20 m after 120 s release, while the neutral gas reaches over 60 m. This may be attributed a vertical

damping of the mixing due to the stable stratification the dense gas release causes.

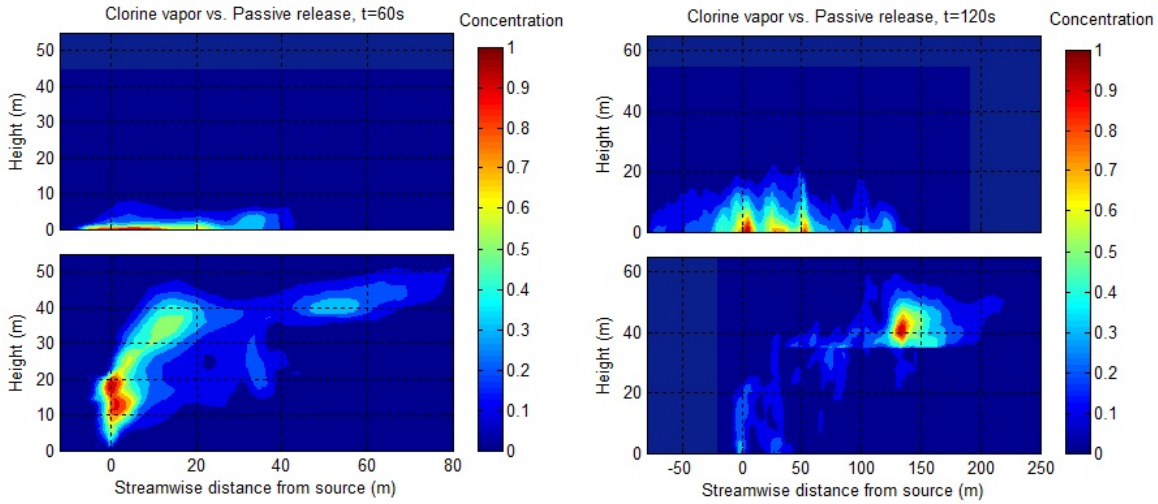

(a) Concentration in a yz-plane at $t = 60s$

(b) Concentration in a yz-plane at $t = 120s$

Figure 4.6 Spatially averaged (in spanwise direction) concentration of chlorine vapor (above) and passive scalar (below)

Figure 4.6 shows the concentration in a yz-plane, i.e., the streamwise distribution of gas, at the same times, $60\ s$ and $120\ s$, as before. Again the top pictures show the chlorine vapor and the ones below the neutral gas. Here, as well, the height difference between the clouds is clearly seen. Another very interesting phenomena can be seen in the contour at the top in Figure 4.6b, where the chlorine vapor is dispersed over $50\ m$ in the opposite direction of the global wind. The same behavior is not seen for the neutral gas. Since the heavy gas keeps close to the ground, it is more affected by the local flow field at ground level and the geometry of the urban area which produce channeling effects.

4.2 Ammonia release

As already mentioned, the results yielded an unexpected difference between the chlorine and ammonia release regarding the evaporation of the liquid state. A possible explanation lies in the latent heat of vaporization for the two chemicals. Liquid ammonia has a much higher latent heat ($1371.2\ kJ/kg$) compared to chlorine ($287.79\ kJ/kg$), which means that for the same temperature difference, a smaller amount will be evaporated. Normally, a lot of the heat required to evaporate the liquid states would come from the ground and the difference between ammonia and chlorine would be less apparent, but this effect is not included in the simulations. This would correspond to a very cold ground temperature in reality.

Even though ammonia in gaseous phase is lighter than air, the liquid phase is heavier than the surrounding air. Also, a mixture of ammonia vapor and air can still be heavier than the surrounding air due to the low temperature which will increase the density of the air in the mixture. Figure 4.7a shows the density of the liquid/vapor ammonia mixture after $60\ s$ release, $1\ m$ above ground.

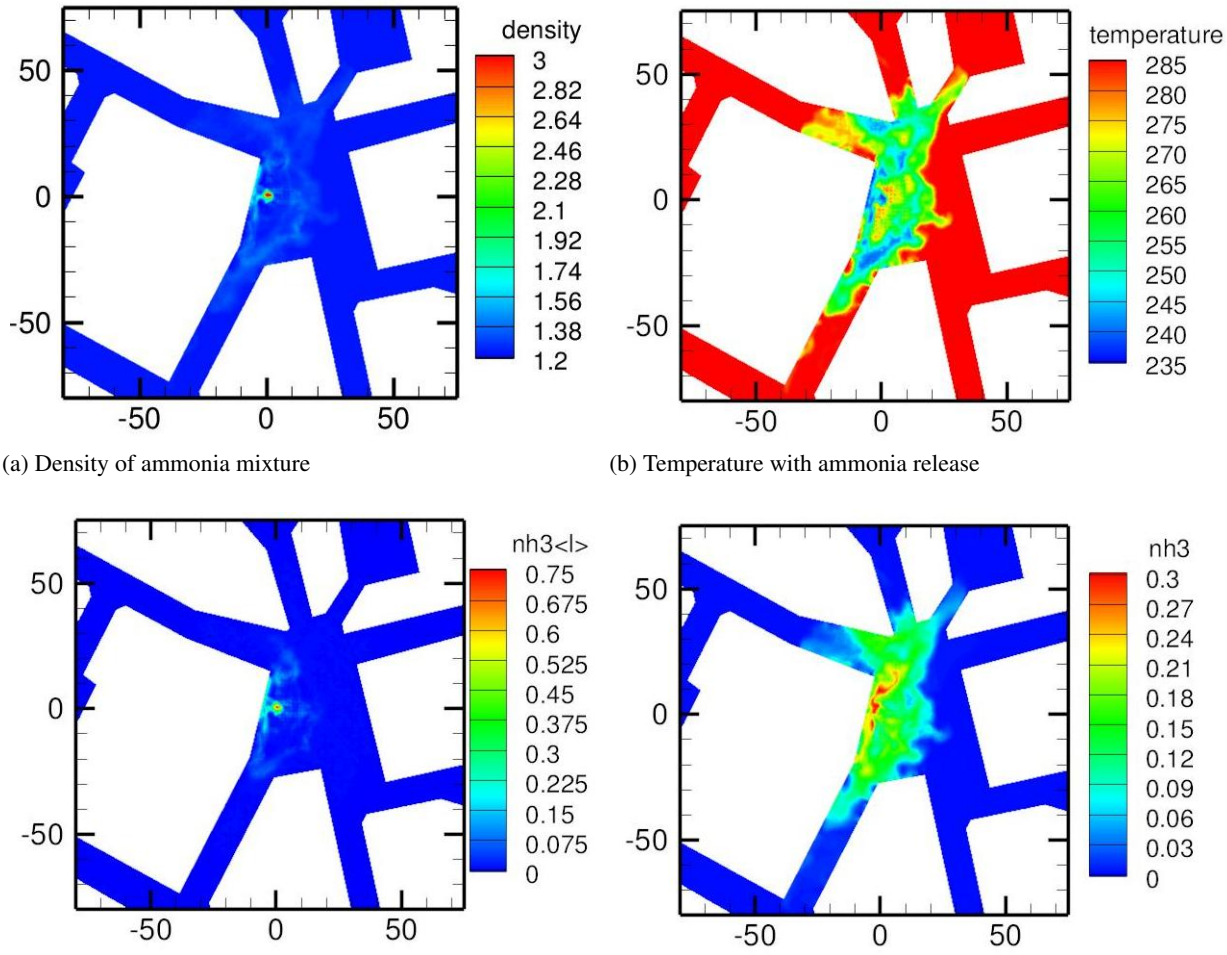

(a) Density of ammonia mixture

(b) Temperature with ammonia release

(c) Concentration of liquid ammonia

(d) Concentration of vaporized ammonia

Figure 4.7 Density and temperature, as well as concentration of liquid and gaseous ammonia, in a plane parallel to the ground at $1\ m$ *height after* $60\ s$ *release*

A much smaller area with high density is observed compared to the chlorine case. These areas are highly correlated to where the highest concentration of liquid ammonia can be found (see figure 4.7c). Also, it is possible to see small areas with density lower than the density of air ($1.225\ kg/m^3$), indicating a high concentration of vaporized ammonia here (see figure 4.7d). Figure 4.7b shows the temperature in the area close to the source. Not only is a larger area affected by temperatures lower than the ambient air temperature with ammonia release compared to chlorine release, but also the absolute value is much lower here. The temperature reaches down to $235\ K$, which is lower than the boiling point of ammonia, and in these areas it is also seen high concentration of the liquid state (see figure 4.7c). An interesting observation is that there is a perfect correspondence between the area covered by vaporized ammonia and area with temperature lower than $288.15\ K$. Hence, the gaseous ammonia did not reach ambient air temperature during the $60\ s$ the release lasted, which vaporized chlorine did (see figure 4.3b and 4.3d).

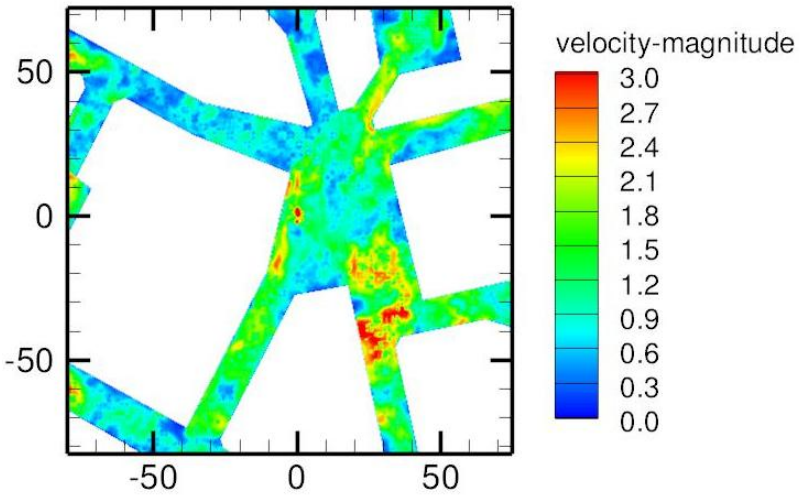

Figure 4.8 Velocity magnitude, close to the source of ammonia release, in a plane parallel to the ground at $1\ m$ *height and* $60\ s$

In section 4.1 it was shown that there was a significant difference in the wind velocity close to the source between release of chlorine and passive gas. Figure 4.8 show how the wind field would look like if ammonia was to be released. Again, the velocity is significantly different from both previous releases. An increase in velocity magnitude is visible in the areas where the concentration of gaseous ammonia is high (and the density is low), indicating that the lighter-than-air gas will give rise to increased wind speeds. This may also lead to an unstable stratification with increased mixing.

4.3 Transport of non-neutral gases

Due to the different evaporation rate between chlorine and ammonia, the sources of the released gaseous states were very different for the two simulations. Hence, a direct comparison can not be made, but a description of each of the dispersion processes will be given. The following pictures show the dispersion of vaporized chlorine and ammonia at three different times.

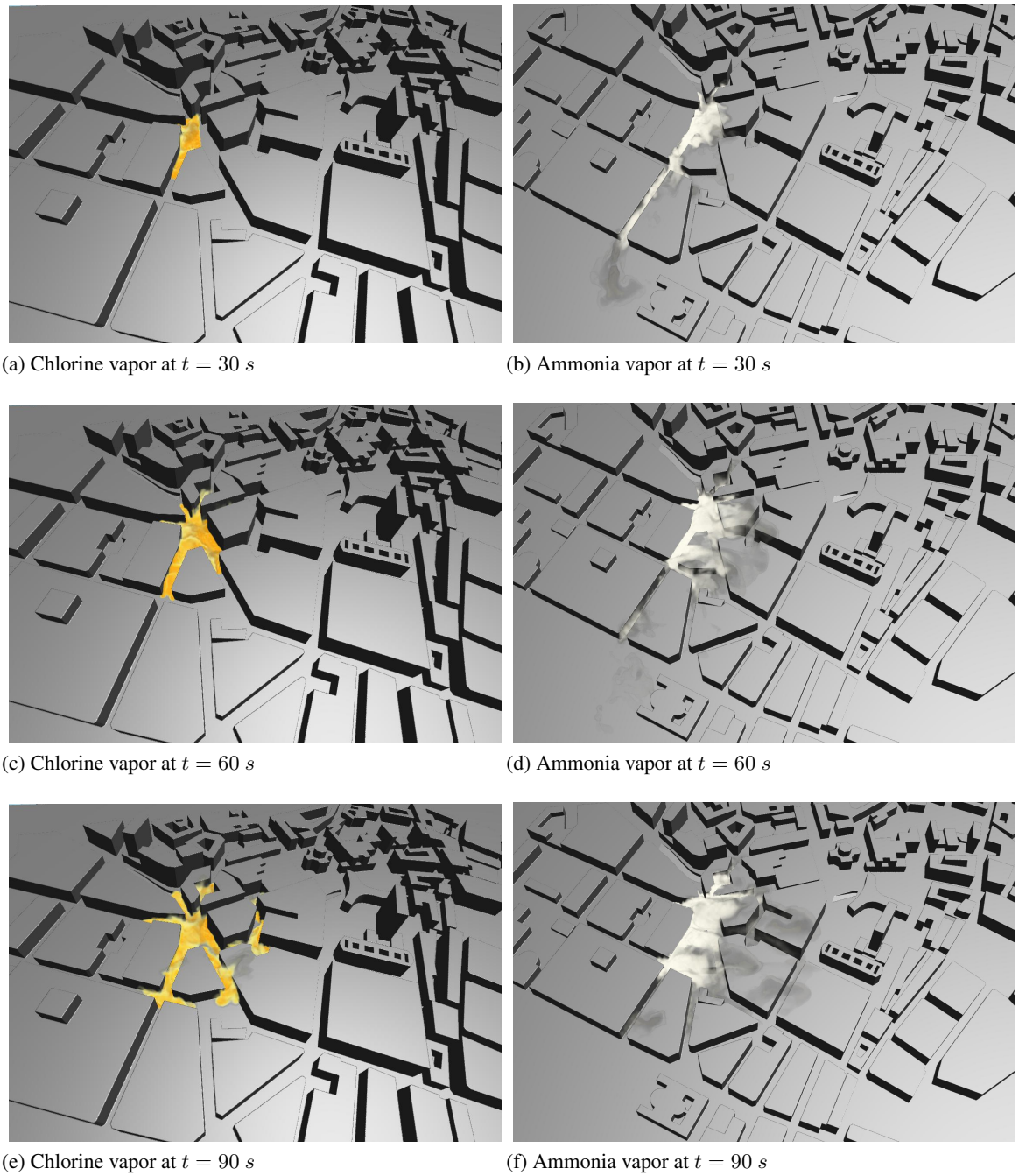

(a) Chlorine vapor at $t = 30\ s$

(b) Ammonia vapor at $t = 30\ s$

(c) Chlorine vapor at $t = 60\ s$

(d) Ammonia vapor at $t = 60\ s$

(e) Chlorine vapor at $t = 90\ s$

(f) Ammonia vapor at $t = 90\ s$

Figure 4.9 Visualization of release and dispersion of chlorine and ammonia gas

Figures 4.9a and 4.9b show the release and dispersion of non-neutral gases after $30\ s$ release time. Here, the discharge of liquid/vapor mixture is still in progress. Chlorine (figure 4.9a) has spread in an area close to the source and most of the vapor is located close to the ground. Ammonia (figure 4.9b) on the other hand covers a larger area, which is not surprising considering the larger area filled with liquid ammonia giving rise to a secondary evaporation. Also, the ammonia cloud reaches higher, an effect caused by the lower density of the gas which induce an increased mixing.

Figures 4.9c and 4.9e show the chlorine gas after $60\ s$ and $90\ s$, respectively. Most of the gas is dispersed within the building blocks, i.e., below the typical building heights. This indicates that the vertical mixing process is subdued which is an effect of the density difference between the heavy chlorine and the lighter surrounding air. This difference, cause stable stratification to arise.

Figures 4.9d and 4.9f show the gaseous phase of ammonia after $60\ s$ and $90\ s$, respectively. High concentrations are found close to the release point, and the dispersion mostly goes in the global wind direction. The light ammonia gas cloud reaches higher than the heavy chlorine cloud. An interesting observation is that the concentration seems to decrease quite rapidly with distance from the source. After $90\ s$ the original source has stopped discharging liquid-vapor mixture, but there is still a lot of liquid ammonia on the ground. This liquid evaporates, yielding a large secondary source. Since ammonia vapor is lighter than air, the density difference will give rise to an increased wind velocity which in turn will increase the mixing process. With increased mixing, the concentration of ammonia will be reduced, i.e., the gas will disperse more but at the same time it will be diluted, which is seen in the pictures.

Consequently, the heavier-than-air gas will induce a stable stratification, leading to reduced mixing, especially in the vertical direction. This leads to a dispersion process where the gas sticks relatively close to the ground and is mostly affected by the local flow field, which in turn is affected by the building structures. Since chlorine has higher density than the surrounding air, it is also able to induce a momentum flux that can, in some places, transport the gas against the local wind. The lighter-than-air ammonia will disperse from a much larger area due to the slower evaporation of the liquid state. Since the density of gaseous ammonia is lower than that of air, it will induce an unstable stratification, yielding an increased vertical mixing process. This, in turn, will disperse the gas more, especially in the vertical direction, but it also causes the concentration to decease since it mixes the ammonia with more air.

5 Concluding remarks

The transport and dispersion of non-neutral gases, as well as a neutral gas, in a complex urban area have been investigated. Previous works indicate that the LES method is well suited for predicting complex flow fields and passive scalar dispersion. Since the flow field is the most dominating effect also when it comes to dispersion of non-neutral scalars, this method was chosen.

A significant difference between the evaporation of chlorine and ammonia was observed, where chlorine evaporated quickly whereas liquid ammonia did not. A possible explanation for this

lies in the latent heat of evaporation. A liquid pool was formed in the latter case. This difference led to a considerable disparity between the sources, where one could be assumed to be a point source (chlorine), while the other (ammonia) let off gas from a much larger area. That affected the subsequent transport and made it hard to compare the two cases of non-neutral gases to each other. Since the neutral case only considers release of gas from a point source, the dispersion of neutral gas can only be compared to transport of chlorine in this study.

Results indicate that the heavier-than-air gas is not as affected by vertical mixing as the neutral gas. This results in a plume that do not reach as high, but as time progresses spread more horizontally compared to the passive scalar. The latter is caused by the channeling effects due to building structures. An analysis of the temperature field confirms a rapid evaporation of the liquid chlorine. No liquid pool was observed and the vaporized chlorine quickly reached the same temperature as the surrounding air.

In the ammonia case, not only the gaseous phase but also the liquid state was transported. Liquid ammonia covered a large area on the ground in the vicinity of the outlet source. This gave rise to secondary evaporation and, hence, a larger release area for ammonia gas. Since the density of gaseous ammonia is lower than the density of air, the local wind speed increased in areas with high concentration of vapor ammonia. This subsequently increased the mixing yielding a higher, but also a more diluted, plume. The dispersed ammonia stayed cold for a longer period of time compared to chlorine. This reduced the density differences between the ammonia and surrounding air.

References

W. J. Coirier, D. M. Fricker, M. Furmanczyk, and S. Kim. A Computational Fluid Dynamics approach for urban area transport and dispersion modeling. *Environmental Fluid Dynamics*, 5: 443–479, 2005.

P. A. Durbin and B. A. Pettersson Reif. The elliptic relaxation method. In B. Launder and N. Sandham, editors, *Closure Strategies for turbulent and transitional flows*. Cambridge University Press, 2002. ISBN 0 521 79208 8.

Fluent 6.3 User's Guide. *Fluent 6.3 User's Guide*. Fluent, Inc., New Hampshire, USA, 2006. /fluent/flug.pdf (or from web).

H. E. Fossum, B. A. Pettersson Reif, M. Tutkun, and T. Gjesdal. On the use of computational fluid dynamics to investigat aerosol dispersion in an industrial environment: A case study. *Boundary-Layer Meteorology*, 144:21–40, 2012.

RL Lee, R. J. Calhoun, S. T. Chan, J. Leone, J. H Shinn, and D. E. Stevens. Urban dispersion cfd modeling, fact or fiction? In *84th AMS meeting, 3rd Symposium on the Urban Environment*, Davis, CA, USA, 2000.

F.-S. Lien and E. Yee. Numerical modelling of the turbulent flow developing within and over a 3d building array, part i: A high-resolution Reynolds-Averaged Navier-Stokes approach. *Boundary-Layer Meteorology*, 112:427–466, 2004.

F.-S. Lien, E. Yee, H. Ji, A. Keats, and K. J. Hsieh. Progress and challenges in the development of physically-based numerical models for prediction of flow and contaminant dispersion in the urban environment. *Int. Journal of Computational Fluid Dynamics*, 20:323–337, 2006.

Y.S. Liu, G.X. Cui, Z.S. Wang, and Z.S. Zhang. Large eddy simulation of wind field and pollutant dispersion in downtown macao. *Atmospheric Environment*, 45:2849–2859, 2011.

M. A. McBride, A. B. Reeves, M. D. Vanderheyden, C. J. Lea, and X. X. Zhou. Use of advanced techniques to model the dispersion of chlorine in complex terrain. *Process Safety Environment*, 79:89–102, 2001.

G. A. Perdikaris and F. Mayinger. Numerical simulation of heavy gas cloud dispersion within topographically complex terrain. *Journal of Loss Prevention in the Process Industries*, 7:391–396, 1994.

J. L. Santiago, A. Martilli, and F. Martin. Cfd simulation of airflow over a regular array of cubes. part i: Three-dimensional simulation of the flow and validation with wind-tunnel experiments. *Boundary-Layer Meteorology*, 122:609–634, 2007.

S. Sklavounos and F. Rigas. Validation of turbulence models in heavy gas dispersion over obstacles. *Journal of Hazardous Materials*, A108:9–20, 2004.